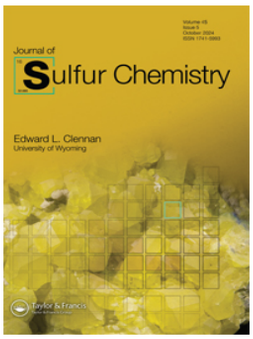

Journal of Sulfur Chemistry

ISSN: (Print) (Online) Journal homepage: www.tandfonline.com/journals/gsrp20

Vachelia nilotica seed-mediated green synthesis of sulfur nanoparticles (SNPs) and evaluation of anticancer & antifungal activities

Pradeep Deshmukh, Yogesh Biradar, Dnyaneshwar Wankhede, Vikas Ragole, Sonaji Gayakwad & Kailas Kadam

To cite this article: Pradeep Deshmukh, Yogesh Biradar, Dnyaneshwar Wankhede, Vikas Ragole, Sonaji Gayakwad & Kailas Kadam (30 Aug 2024): *Vachelia nilotica* seed-mediated green synthesis of sulfur nanoparticles (SNPs) and evaluation of anticancer & antifungal activities, Journal of Sulfur Chemistry, DOI: 10.1080/17415993.2024.2393391

To link to this article: https://doi.org/10.1080/17415993.2024.2393391

Published online: 30 Aug 2024.

JOURNAL OF SULFUR CHEMISTRY
https://doi.org/10.1080/17415993.2024.2393391

Taylor & Francis
Taylor & Francis Group

Vachelia nilotica seed-mediated green synthesis of sulfur nanoparticles (SNPs) and evaluation of anticancer & antifungal activities

Pradeep Deshmukh[a], Yogesh Biradar[a], Dnyaneshwar Wankhede [a], Vikas Ragole[b], Sonaji Gayakwad[c] and Kailas Kadam[d]

[a]School of Chemical Sciences, Swami Ramanand Teerth Marathwada University, Nanded, India; [b]Late Ramesh Warpudkar ACS College Sonpeth, Parbhani, India; [c]Department of Chemistry, Mrs. K.S.K. College, Beed, India; [d]Department of Chemistry and Research Center, Padmashri Vikhe Patil College, Ahmednagar, India

ABSTRACT

Sulfur nanoparticles (SNPs) have been successfully synthesized by applying *Vachelia nilotica* seed extract as a bioactive aqueous material by a disproportionation reaction of sodium thiosulfate pentahydrate ($Na_2S_2O_3{\cdot}5H_2O$) with a 10% hydrochloric acid (HCl) at room temperature. The synthesized SNPs were characterized by UV–Visible, Fourier Transfer Infrared (FTIR) spectroscopy, Scanning Electron Microscopy (SEM), Transmission Electron Microscopy (TEM), Energy-Dispersive X-ray Spectroscopy (EDS), and X-ray Diffraction (XRD) techniques. The usual size of SNPs was determined by an XRD study and calculated with the Debye–Scherrer formula. The SNPs are crystalline with a calculated average size of 45 nm. The SEM and TEM analyses revealed spherical shape and size around 55 nm of SNPs. The synthesized SNPs were screened for their antifungal activity against *M. furfur* species and for anticancer activities against *(MCF-7, HepG2)* cell lines. The obtained results suggested towards moderate to good antifungal and excellent anticancer activities.

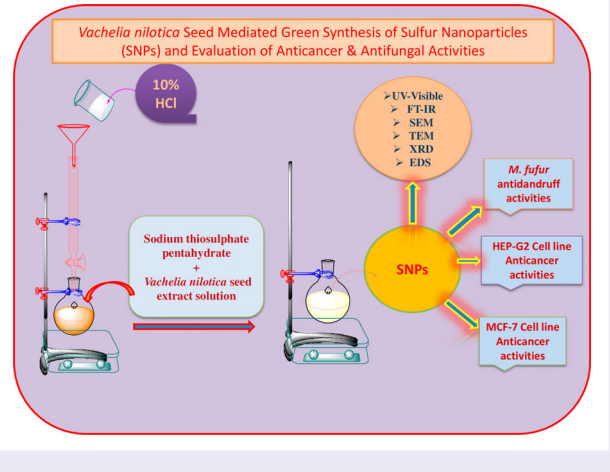

ARTICLE HISTORY
Received 31 January 2024
Accepted 11 August 2024

KEYWORDS
Vachelia nilotica; sulfur nanoparticles (SNPs); anticancer; antifungal; *M. furfur*

CONTACT Dnyaneshwar Wankhede dswchem@srtmun.ac.in, dswchem@yahoo.co.in

1. Introduction

Nanoparticles are inorganic materials with specific characteristics such as size, distribution, chemical composition, and morphology containing structural dimension measuring 1–100 nanometers. Nanoparticles with greater surface area to volume ratio compared to that of bulk materials have gained enormous attention of researchers from various fields including chemistry, physics, material sciences, life sciences, medicinal fields, agriculture, biotechnology, food and safety, cosmetics, industrial area, and engineering. The high interest in nanoparticles is also because of their unique optical, magnetic, electronic, and catalytic properties with their distinctive feature of size and shape [1,2].

The application of various dyes in industrial application has created a major concern regarding environmental safety as these dyes are one of the main water pollutants and critical threats to environment and human health. Nanoparticles and nanocomposites are promising remedies for the degradation of these organic dyes from wastewaters as they can convert these toxic pollutants into non-toxic compounds under light. Thus photocatalytic degradation using nanomaterials is an important research area these days and many researchers have contributed [3–9].

Physical and chemical methods of nanoparticles synthesis have disadvantages such as high cost, environmentally hazardous chemicals, and non-availability for medical applications due to the presence of toxic capping agents which has prompted researchers to use green methods of synthesis [10,11]. The green methods emphasize on the synthesis of nanoparticles for maximum societal benefit, with minimal impact on the ecosystem [12–14]. In this regard, most of the researchers from academic and industry backgrounds have focused on applications of biological materials such as plants, marine algae, fungi, and bacteria for the green synthesis of nanoparticles [15–22]. In recent years, many researchers have synthesized metallic and non-metallic nanoparticles [23–30], metal oxide nanoparticles and nanocomposites [4–9,31–38] using green methods.

The use of seed powder aqueous extract of various plants for the synthesis of metallic nanoparticles such as silver [39,40], gold [41,42], copper [43], magnesium [44], and so on is well documented, but no such report is available in case of SNPs synthesis. Thus, in present investigation, we report the synthesis of SNPs using the seed powder aqueous extract of the *Vachelia nilotica*, a plant with large number of medicinal properties [45]. The *Vachelia nilotica* seed powder aqueous extract contains various phytochemicals that actively participate as reducing and capping agent to generate and stabilize the SNPs by converting the S^{2}- to S^{0} state [46]. The shape, size, and crystalline nature of synthesized 'green' SNPs are defined by Scanning Electron Microscopy (SEM), Transmission Electron Microscopy (TEM), Energy-Dispersive X-ray Spectroscopy (EDS), and X-ray Diffraction (XRD) analytical methods. The biomolecules attached to the SNPs on the surface are responsible for their reduction as well as stabilization and are identified by UV–visible and FT-IR techniques. The synthesized SNPs were tested for their antifungal and anticancer activities and observed to exhibit good antifungal and excellent anticancer activities.

2. Results and discussion

2.1. UV–Visible spectroscopy

The UV–Visible absorption spectral studies were carried out to confirm the formation of SNPs using *Vachelia nilotica* seed extract solution (Figure 1a). After completion of

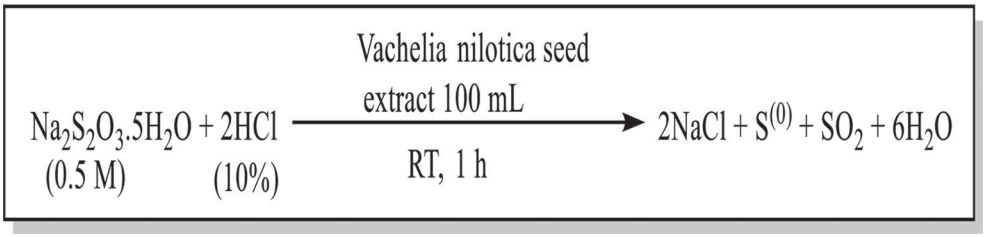

Figure 1. (a) UV–Visible spectrum of *Vachelia nilotica* aqueous seed extract solution and (b) UV–Visible spectrum of synthesized SNPs.

reaction, the samples were subjected to record absorption peaks for the SNPs (Figure 1b). The UV–Visible spectrum recorded in the range of 200–800 nm for *Vachelia nilotica* seed extract solution exhibited peaks at 207.11 and 261.46 nm indicating the presence of different phytochemicals like fatty acids, terpenoids, alkaloids, and phenolic compounds. The sample solution exhibited absorption peak at 264.24 nm indicating the presence of SNPs. Reports indicating the presence of SNPs in the range of 250–300 nm with maximum absorbance at 264 nm wavelength [49] are available.

2.2. Fourier Transform Infrared (FT-IR) analysis

FT-IR data readings are performed to find out the possible biomolecules accountable for the reduction, capping, and efficacious stabilization of SNPs. FT-IR spectrum of *Vachelia nilotica* aqueous seeds extract solution is illustrated in (Figure 2a). It was observed that the groups responsible for the formation of the SNPs were –OH (3321 cm^{-1}), –C = O (1365 cm^{-1}), and C–O–C (1042 cm^{-1}). These functional groups act as dispersing, capping, and stabilizing agents for SNPs during synthesis.

The analysis of FT-IR spectrum of SNPs (Figure 2b) clearly indicated the presence of peak at 465 cm^{-1} due to SNPs. These results show that the reaction took place and nanoparticles were formed. The spectrum indicated a new chemistry linkage on the surface of the SNPs and is an enough evidence in favor of binding of *Vachelia nilotica* aqueous seeds extract to SNPs acting as a stabilizer and dispersing agent to prevent agglomeration of SNPs [50].

2.3. X-ray Diffraction analysis

The XRD pattern of synthesized SNPs by *Vachelia nilotica* aqueous seed extract illustrated in Figure 3 exhibited sharp peaks indicating bigger crystals. The 2θ peaks observed at 21.02°, 22.13°, 25.77°, 26.02°, 27.87°, 28.71°, 31.49°, 34.28°, 37.07°are attributed to the crystal planes of sulfur at (113), (222), (133), (026), (311), (206), (313), (044), and (244) respectively [51,52]. The formation of SNPs also involves sodium chloride formation as a side product and the extra peaks at 42.92°, 47.80°, and 51.03° can be attributed to the crystal planes of sodium chloride at (404), (319), and (515) respectively. The results indicated that SNPs are well crystalline and the position and relative intensity of the diffraction peaks match well with the standard monoclinic phase sulfur diffraction pattern [JCPDSN-34-094]. The crystal planes corresponding to the peaks are indicated in Figure 3.

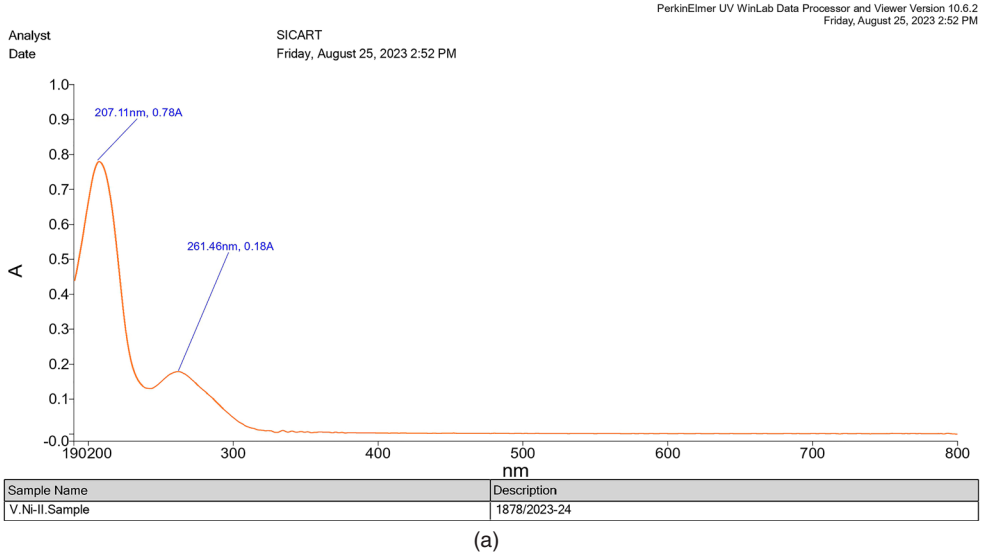

(a)

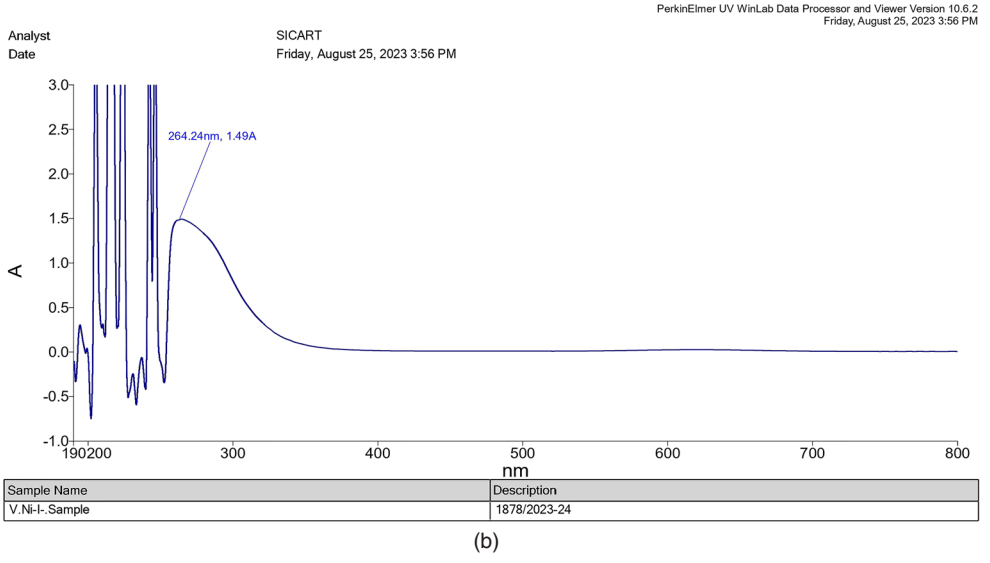

(b)

Figure 2. (a) The FT-IR spectrum of *Vachelia nilotica* aqueous seed extract solution and (b) the FT-IR spectrum of synthesized SNPs.

The particle size of the synthesized SNPs was calculated using the Debye–Scherrer formula [8,9,53,54], $D = K\lambda/(\beta\cos\theta)$, where $D =$ the nanoparticles crystalline size, $K =$ Scherrer constant (0.90), $\lambda =$ wavelength 1.54 A°, $\beta =$ full width at half maximum (FWHM), and $\theta =$ half diffraction angle or Bragg angle or peak position (radians). The crystallite size was estimated to be 45 nm using the diffraction peak associated with crystal plane (222).

2.4. Scanning Electron Microscopy analysis

Scanning Electron Microscopy or SEM is useful in determining topography of materials and provides detailed surface data of solid samples. In present investigation, the SEM

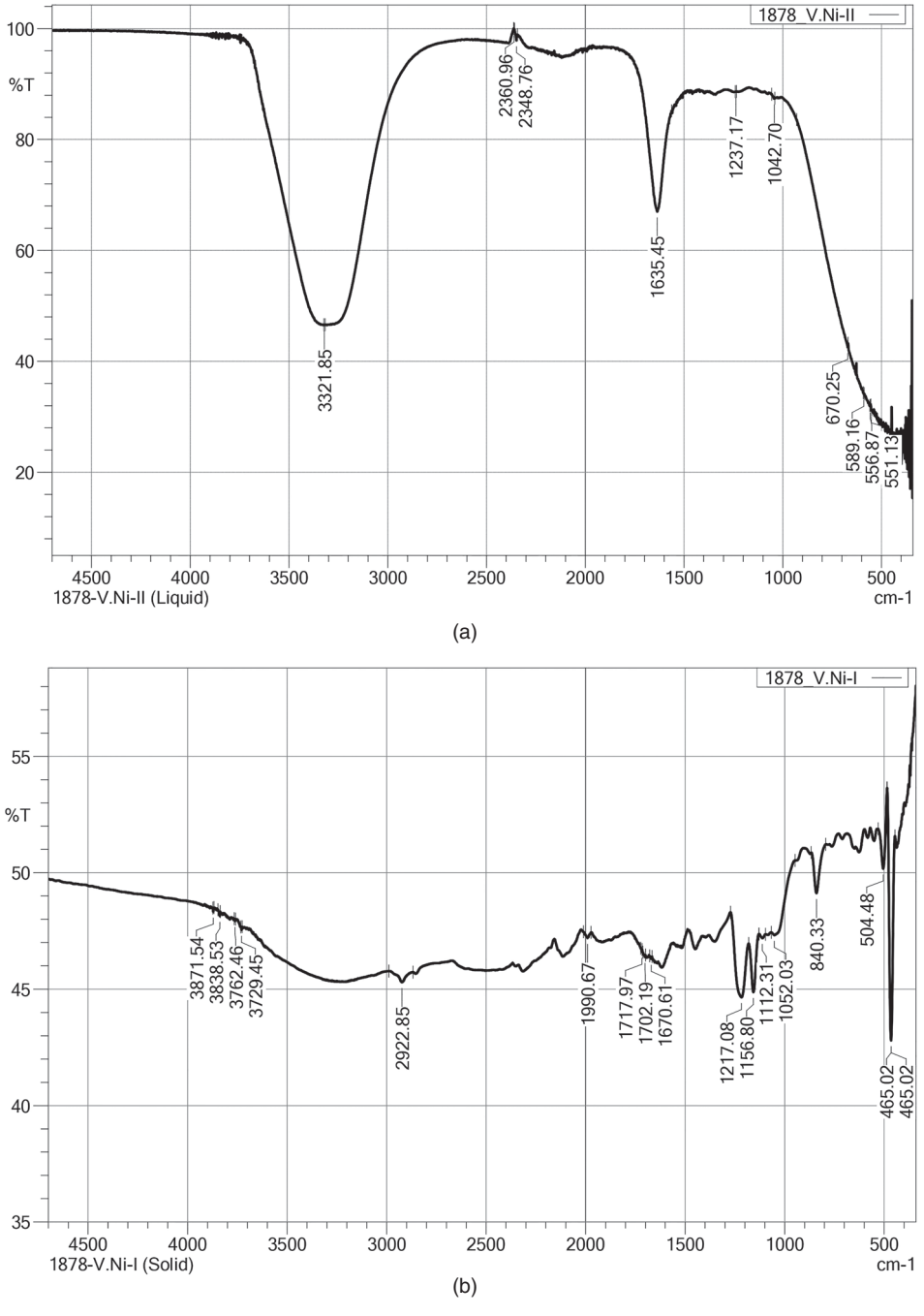

Figure 3. The XRD pattern of synthesized SNPs.

images indicated that synthesized SNPs are almost spherical in shape and were of uniform size (Figure 4) [55]. Figure 4 indicated that the SNPs obtained using aqueous seed extract solution are having uniform particle size, spherical, and having tendency to prevent agglomeration. This is enough evidence to emphasize the role of aqueous seed extract

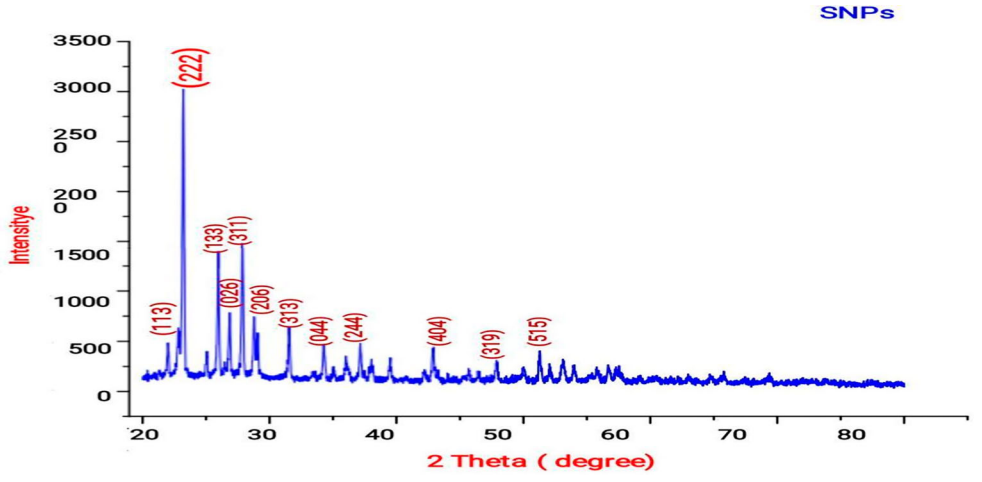

Figure 4. The SEM images of SNPs.

Table 1. The elemental analysis of SNPs.

S. no.	Test parameter	Name of the instrument	Results (%)	
1	CHNS (%)	CHNS/O Analyzer, Elementar, Unicube	Carbon	1.37
			Hydrogen	4.125
			Nitrogen	0.13
			Sulphur	5.091

solution of *Vachelia nilotica* in the reduction of sulfur and in the formation and stabilization of SNPs [56].

2.5. Transmission Electron Microscopy analysis

Transmission Electron Microscopy or TEM technique is used preferentially in case of nanoparticles to measure particle size, size distribution, and morphology. It is having better resolution than SEM. In present investigation, the TEM images represented that the SNPs are spread homogeneously and the size of the SNPs observed to be 5–100 nm (Figure 5) [24,57].

2.6. Energy-Dispersive X-ray Spectroscopy analysis

EDS is an analytical technique used for chemical characterization or elemental analysis of SNPs which provided information on the chemical composition, phase identification, and required purity of the biosynthesized SNPs [57]. The obtained results are represented in Table 1.

3. Biological activity

3.1. Antidandruff

The results of the antidandruff activities of the SNPs against *M. furfur* species were determined by the Agar well diffusion method. Samples showed moderate to good inhibition

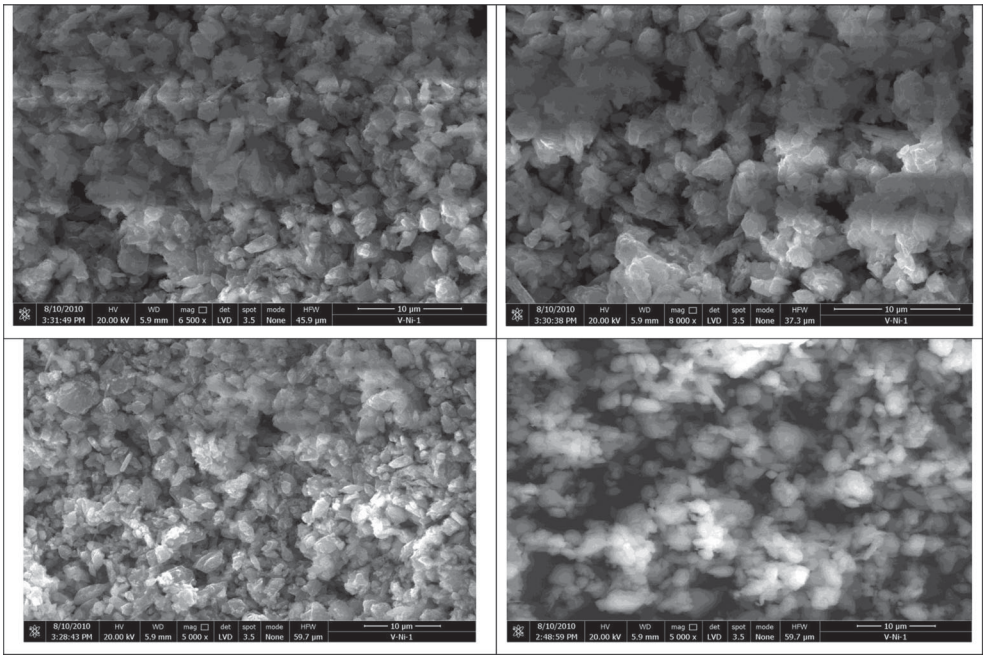

Figure 5. The TEM images of SNPs.

Table 2. Antidandruff activities of the SNPs against *M. furfur* species.

S. no.	Sample	Concentration	Zone of inhibition
1.	Control	–	–
2.	Standard	1 mg/mL	20
3.	SNPs	5 mg/mL	10
		10 mg/mL	14

to the growth of fungal strain *M. Furfur* (Figure 6) [58,59] in comparison to standard. Table 2 represents the results obtained for antidandruff activity. The inhibition was directly proportional with increasing concentration of SNPs.

3.2. Anticancer

The synthesized SNPs exhibited moderate inhibition of cancer cells against *MCF-7* (Breast Cancer Cell Line) and *Hep-G2* (Liver Cancer Cell Line) when compared to standard drug 5-Fluorouracil (5-FU). The synthesized SNPs, however, exhibited lower IC_{50} values compared to that of standard drug 5-FU. This indicated lower concentration required for the killing of 50 percent of cancer cells, thus indicating potential of synthesized SNPs as anticancer agent in comparison to standard 5-FU [60,61]. Tables 3 and 4 represent effects of synthesized SNPs against MCF-7 and Hep-G2 cell lines.

Previous studies have established that the depletion of copper in the cells by chelating agents is a promising strategy to improve cancer therapy and SNPs are able to detain copper [62,63]. Thus SNPs are able to inhibit the growth of cancer cells via inactivation of the MEK/ERK pathway followed by deceleration of mitosis in cancer cells [64,65]. In

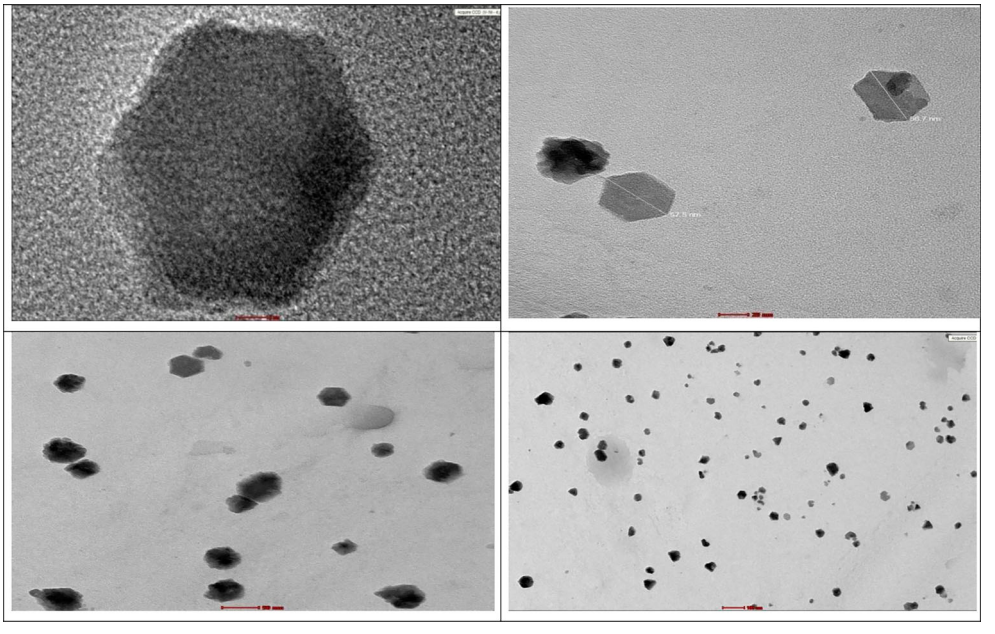

Figure 6. The antidandruff analysis of SNPs.

Table 3. Effects of SNPs against *MCF-7* (Breast cancer cell line) by MTT assay.

S. No.	Sample	Concentration (µg/mL)	OD	Mean	Percentage inhibition (%)	IC_{50}
1.	Control DMSO (0.2% in PBS)		1.1101.1211.113	1.114		
2.	Standard 5FU	10	0.3550.3410.352	0.349	68.67	40.81
		40	0.2840.2740.261	0.273	75.49	
		100	0.1950.1810.191	0.189	83.03	
3.	SNPs	10	0.5400.5560.542	0.546	50.98	34.64
		40	0.4100.4120.411	0.411	63.10	
		100	0.3550.3570.347	0.353	68.31	

Table 4. Effects of SNPs against *Hep-G2* (Liver cancer cell line) by MTT assay.

S. No.	Sample	Concentration (µg/mL)	OD	Mean	Percentage inhibition (%)	IC_{50}
1.	Control DMSO (0.2% in PBS)		0.9850.9760.973	0.978		
2.	Standard5FU	10	0.3550.3460.341	0.347	64.51	43.16
		40	0.2860.2860.272	0.281	71.26	
		100	0.1920.1830.175	0.183	81.28	
3.	SNPs	10	0.4890.4810.467	0.479	51.02	35.03
		40	0.3830.3730.370	0.375	61.65	
		100	0.3380.3240.319	0.327	66.56	

present investigation, the anticancer activity effect of SNPs can be dedicated to similar reason.

4. Conclusion

A facile, without surfactant, green route for synthesizing sulfur nanoparticles (SNPs) from sodium thiosulfate pentahydrate ($Na_2S_2O_3{\cdot}5H_2O$) in the presence of *Vachelia nilotica* aqueous seed extract solution was developed. The synthesized nanoparticles were characterized by UV-visible, FT-IR, SEM, TEM, EDS and powder XRD techniques. The results indicated a spherical shape of SNPs with an average size diameter of 55 nm. The SNPs exhibited lower IC_{50} values compared to that of standard 5-Fluorouracil (5-FU) and are thus potential anticancer agents against *MCF-7* (Breast Cancer) & *Hep-G2* (Liver cancer) cell lines.

5. Experimental

5.1. Materials

Vachelia nilotica plant seeds were procured at the Swami Ramanand Teerth Marathwada University Nanded, Maharashtra State, India. Sodium thiosulfate pentahydrate (AR) ($Na_2S_2O_35H_2O$, 99.5%), 10% hydrochloric acid (AR), and rectified spirit (AR) were purchased from S. D. Fine Chemicals Pvt. Ltd. India. All chemicals were used as received.

5.2. Preparation of seed extract

Vachelia nilotica seeds were washed thoroughly with tap water and then with deionized water until all the unwanted visible dirt particles were removed. Subsequently, the seeds were dried and powdered through mortar and pestle. The fine powder measured about 20 g poured into 100 mL deionized water in a 200 mL Erlenmeyer flask. The mixture was boiled at 75–80°C for 2 h and filtered using Whatmann No.1 filter paper to remove solid particles. Then the extract was centrifuged through centrifugation at 5000 rpm for 15 min to remove heavy bioactive materials. The filtrate was stored under low temperature for further experimental work.

5.3. Phytochemical screening of Vachelia nilotica seeds extract

A simple classification system divided phytochemicals into three chemically distinct groups. They are the phenolics, terpenes, N, and S containing compounds. All determinations were done in triplicates [47,48]. In present investigation, the phytochemical screening results indicated the presence of alkaloids, phenolic compounds, terpenoids, and fatty acids in the extract solution.

5.4. Synthesis of sulfur nanoparticles (SNPs)

All the glasswares were cleaned using an aqua regia solution (1:3 nitric acid and hydrochloric acid mixture) to remove the potential nucleation sites on the surface of the glassware before the synthesis.

Sodium thiosulfate pentahydrate [12.406 g/mol (0.5 M)] was dissolved in 100 mL aqueous brick-red seed extract directly and made a homogeneous mixture. After 5 min of

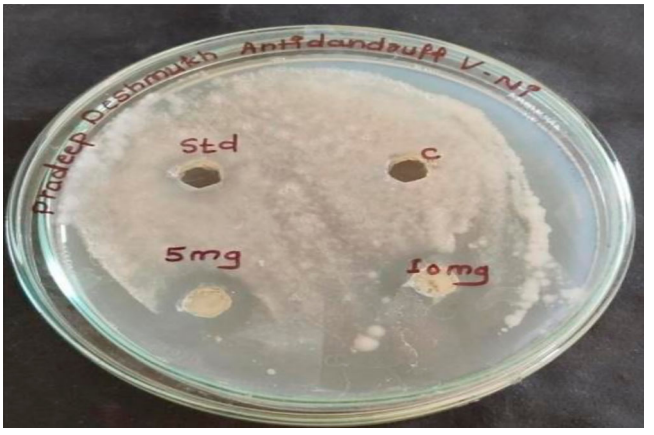

Figure 7. General reaction for synthesis of SNPs.

continuous stirring, 50 mL of 10% hydrochloric acid was added to the homogeneous reaction mixture. During reaction the brick-red colored solution changed to Whitish-yellow precipitate. The whitish-yellow precipitate thus formed was collected and then washed with deionized water and transferred to centrifugation process at 5000 rpm for 30 min under ambient temperature. The supernatant was discarded and the precipitate was repeatedly washed with distilled water and absolute ethanol to get rid of any biological material. The product was finally dried in a vacuum oven at 50°C for 30 min. The general reaction representing formation of SNPs is represented in Figure 7.

5.5. Characterization of sulfur nanoparticles

The response of sulfur nanoparticles to UV range of electromagnetic radiations was determined through recording UV–VIS spectrum (Perkin Elmer; Lambda 1050+ instrument). The FT-IR spectrum recorded (Shimadzu, IR SPIRI instrument) was used to examine synthesized SNPs. The morphology and size distribution of SNPs were determined using SEM (FEI-Nova Nano SEM 450 instrument) and TEM (TALOS F 200I FEG TEM). The crystalline structure of SNPs was characterized by XRD (Rigaku MiniFlex-II instrument) with Cu-K_α ($\lambda = 1.542$ Å) radiation. Purity and chemical composition of the fabricated nanomaterials thus obtained were analyzed with Energy-Dispersive X-ray Spectroscopy (EDS/EDAX) using CHNS/O Analyzer, Elementary, Unicube instrument.

Disclosure statement

No potential conflict of interest was reported by the author(s).

Funding

Authors Pradeep Deshmukh and Yogesh Biradar acknowledge the financial support of Chhatrapati Shahu Maharaj Research, Training and Human Development Institute (SARTHI) Junior Research Fellowship (JRF), Pune, Maharashtra State, India, to carry out this research work.

ORCID

Dnyaneshwar Wankhede http://orcid.org/0000-0002-5787-1013

References

[1] Kharissova OV,Dias HR, Kharisov BI, et al. The greener synthesis of nanoparticles. Trends Biotechnol 2013;31(4):240–248. doi:10.1016/j.tibtech.2013.01.003
[2] Mughal B, Zaidi SZ, Zhang X, et al. Biogenic nanoparticles: synthesis, characterisation and applications. Appl Sci. 2021;11(6):2598. doi:10.3390/app11062598
[3] Far BF, Naimi-Jamal MR, Jahanbakhshi M, et al. Decontamination of Congo red dye from aqueous solution using nanoclay/chitosan-graft gelatin nanocomposite hydrogel. J Mol Liq. 2024;395:123839. doi:10.1016/j.molliq.2023.123839
[4] Fardood ST, Zare FY, Moradnia F, et al. Preparation, characterization and photocatalysis performances of supermagnetic $MgFe_2O_4$@CeO_2 nanocomposites: synthesized via an easy and green sol-gel method. J Rare Earths. 2024. (Published Online). doi:10.1016/j.jre.2024.03.006
[5] Fardood ST, Moradnia F, Zare FY, et al. Green synthesis and characterization of α-Mn_2O_3 nanoparticles for antibacterial activity and efficient visible-light photocatalysis. Sci Rep. 2024;14:6755. doi:10.1038/s41598-024-56666-2
[6] Moradnia F, Fardood ST, Zarei A, et al. Green synthesis of nickel oxide nanoparticles using plant extracts: an overview of their antibacterial, catalytic, and photocatalytic efficiency in the degradation of organic pollutants. Iranian J Catalysis (IJC). 2024;14(1):1–24.
[7] Kiani MT, Ramazani A, Rahmani S, et al. Green synthesis and characterization of superparamagnetic $Cu_{0.25}Zn_{0.75}Fe_2O_4$ nanoparticles and investigation of their photocatalytic activity. Int J Environ Anal Chem. 2022 May 22. (Published Online).
[8] Kiani MT, Ramazani A, Fardood ST. Green synthesis and characterization of Ni0.25Zn0.75Fe_2O_4 magnetic nanoparticles and study of their photocatalytic activity in the degradation of aniline. Appl Organomet Chem. 2023;37(4):e7053. doi:10.1002/aoc.7053
[9] Fardood ST, Moradnia F, Forootan R, et al. Facile green synthesis, characterization and visible light photocatalytic activity of $MgFe_2O4$@$CoCr_2O_4$ magnetic nanocomposite. J Photochem Photobiol A. 2022;423:113621. doi:10.1016/j.jphotochem.2021.113621
[10] Chaudhuri RG, Paria S. Synthesis of sulphur nanoparticles in aqueous surfactant solutions. J Colloid Interface Sci. 2010;343(2):439–446. doi:10.1016/j.jcis.2009.12.004
[11] Bhat MI, Singh S, Thapliyal U. Green nanomaterials: importance and applications. In: Chakraborty I, Hakeem KR, editors. Green nanomaterials in energy conversion and storage applications 2024 (pp. 17–44). Palm Bay, FL: Apple Academic Press.
[12] Surendranath A, Mohanan PV. Impact of nanoparticles in balancing the ecosystem. Biointerface Res Appl Chem. 2020;11:10461–10481. doi:10.33263/BRIAC113.1046110481
[13] Shah SN, Shah Z, Hussain M, et al. Hazardous effects of titanium dioxide nanoparticles in ecosystem. Bioinorg Chem Appl. 2017;2017:4101735.
[14] Khan MR, Akram M. Nanoparticles and their fate in soil ecosystem. In: Biogenic nano-particles and their use in agro-ecosystems. 2020. p. 221–245
[15] Dikshit PK, Kumar J, Das AK, et al. Green synthesis of metallic nanoparticles: applications and limitations. Catalysts. 2021;11(8):902. doi:10.3390/catal11080902
[16] AlNadhari S, Al-Enazi NM, Alshehrei F, et al. A review on biogenic synthesis of metal nanoparticles using marine algae and its applications. Environ Res 2021;194:110672.
[17] Alprol AE, Mansour AT, Abdelwahab AM, et al. Advances in green synthesis of metal oxide nanoparticles by marine algae for wastewater treatment by adsorption and photocatalysis techniques. Catalysts. 2023;13(5):888. doi:10.3390/catal13050888
[18] Aswathi VP, Meera S, Maria CA, et al. Green synthesis of nanoparticles from biodegradable waste extracts and their applications: a critical review. Nanotechnol Environ Eng. 2023;8(2):377–397. doi:10.1007/s41204-022-00276-8

[19] Baloch H, Siddiqua A, Nawaz A, et al. Synthesis and characterization of sulphur nanoparticles of citrus limon extract embedded in nanohydrogel formulation: in vitro and in vivo studies. Gels. 2023;9(4):284.
[20] Ashengroph M, Daj S. Green synthesis and characterization of silver sulfide nanoparticles using bacillus safensis strain GMS10 isolated from contaminated soil of gold mine. Appl Biol. 2023;35(4):7–24.
[21] Ghotekar S, Pagar T, Pansambal S, et al. A review on green synthesis of sulphur nanoparticles via plant extract, characterization and its applications. Adv J Chem-Sect B. 2020;2(3):128–143.
[22] Nam NT, Truong DP, An TT, et al. Biological activity prospects of selenium-decorated graphene oxide composite by green synthesis using *Sesbania sesban* flower extract. Diam Relat Mater. 2024;141:110563. doi:10.1016/j.diamond.2023.110563
[23] Patel P, Vadalia J, Butani K, et al. Green synthesis of silver nanoparticles, characterization and their biological efficacy. Nanotechnol In Silico Tools. 2024: 117–139.
[24] Javan Kouzegaran V, Farhadi K. Green synthesis of sulphur nanoparticles assisted by an herbal surfactant in aqueous solutions. Micro Nano Lett. 2017;12(5):329–334. doi:10.1049/mnl.2016.0567
[25] Chaudhary J, Tailor G, Yadav M, et al. Green route synthesis of metallic nanoparticles using various herbal extracts: a review. Biocatalysis Agric Biotechnol. 2023;50:102692.
[26] Bordiwala RV. Green synthesis and applications of metal nanoparticles. A review article. Results Chem. 2023;5:100832.
[27] Rani N, Singh P, Kumar S, et al. Plant-mediated synthesis of nanoparticles and their applications: a review. Mater Res Bull. 2023;163:112233.
[28] Lesnichaya M, Gazizova A, Perfileva A, et al. Starch-capped sulphur nanoparticles synthesized from bulk powder sulphur and their anti-phytopathogenic activity against *Clavibacter sepedonicus*. IET Nanobiotechnol. 2021;15(7):585–593. doi:10.1049/nbt2.12044
[29] Shankar S, Jaiswal L, Rhim JW. New insight into sulphur nanoparticles: synthesis and applications. Crit Rev Environ Sci Technol. 2021;51(20):2329–2356. doi:10.1080/10643389.2020.1780880
[30] Muralidharan VA, Ramesh S, Muthukrishnan L. Facile fabrication of *Annona squamosa* L. seed extract mediated silver nanoparticles challenged against biofilm forming oral pathogens. Plant Nano Biology. 2023;3:100023. doi:10.1016/j.plana.2022.100023
[31] Fardood ST, Ramazani A, Joo SW. Green chemistry approach for the synthesis of copper oxide nanoparticles using tragacanth gel and their structural characterization. J Struct Chem. 2018;59(2):482–486. doi:10.1134/S0022476618020324
[32] Chandrasekaran R, Patil S, Krishnan M, et al. The characteristics of green-synthesized magnesium oxide nanoparticles (MgONPs) and their biomedical applications. Mini Rev Med Chem. 2023;23(9):1058–1069. doi:10.2174/1389557523666221212114416
[33] Bukhari SA, Shakir HA, Khan M, et al. Biosynthesized cerium oxide nanoparticles CeO_2NPs: recent progress and medical applications. Curr Pharm Biotechnol. 2023;24(6):766–779. doi:10.2174/1389201023666220821161737
[34] Periakaruppan R, Selva Kumar T, Vanathi P, et al. Phyto-synthesis and characterization of parthenium-mediated iron oxide nanoparticles and an evaluation of their antifungal and antioxidant activities and effect on seed germination. JOM. 2023;75(12):5235–5242. doi:10.1007/s11837-023-05760-3
[35] Rajeshkumar S, Parameswari RP, Sandhiya D, et al. Green synthesis, characterization and bioactivity of mangifera indica seed-wrapped zinc oxide nanoparticles. Molecules. 2023;28(6):2818. doi:10.3390/molecules28062818
[36] Ahmad B, Khan MI, Naeem MA, et al. Green synthesis of NiO nanoparticles using Aloe vera gel extract and evaluation of antimicrobial activity. Mater Chem Phys. 2022;288:126363. doi:10.1016/j.matchemphys.2022.126363
[37] Waghchaure RH, Adole VA. Biosynthesis of metal and metal oxide nanoparticles using various parts of plants for antibacterial, antifungal and anticancer activity: a review. J Indian Chem Soc. 2023;100(5):100987.

[38] Gebre SH. Bio-inspired synthesis of metal and metal oxide nanoparticles: the key role of phytochemicals. J Cluster Sci. 2023;34(2):665–704. doi:10.1007/s10876-022-02276-9
[39] Wang C, Rong Z, Wang J, et al. Seed-mediated synthesis of high-performance silver-coated magnetic nanoparticles and their use as effective SERS substrates. Colloids Surf A. 2016;506:393–401. doi:10.1016/j.colsurfa.2016.05.103
[40] Bhattacharjee RR, Dasgupta U. Seed-mediated synthesis of silver nanoparticles: tunable surface plasmon and their facile fabrication. Mater Today Proc. 2021;43(2):1342–1347. doi:10.1016/j.matpr.2020.09.167
[41] Jenkins JA, Wax TJ, Zhao J. Seed-mediated synthesis of gold nanoparticles of controlled sizes to demonstrate the impact of size on optical properties. J Chem Educ. 2017;94(8):1090–1093. doi:10.1021/acs.jchemed.6b00941
[42] Leng W, Pati R, Vikesland PJ. Room temperature seed mediated growth of gold nanoparticles: mechanistic investigations and life cycle assessment. Environ Sci: Nano. 2015;2:440–453. doi:10.1039/C5EN00026B
[43] Lu LM, Zhang XB, Shen GL, et al. Seed-mediated synthesis of copper nanoparticles on carbon nanotubes and their application in nonenzymatic glucose biosensors. Anal Chim Acta. 2012;715:99–104. doi:10.1016/j.aca.2011.12.011
[44] Lomonosov V, Hopper ER, Ringe E. Seed-mediated synthesis of monodisperse plasmonic magnesium nanoparticles. Chem Commun. 2023;59:5603–5606. doi:10.1039/D3CC00958K
[45] Ali A, Akhtar N, Khan BA, et al. Acacia nilotica: a plant of multipurpose medicinal uses. J Med Plants Res. 2012 Mar 9;6(9):492–496.
[46] Abduljawad EA. Review of some evidenced medicinal activities of *Acacia nilotica*. Archiv Pharmacy Pract. 2020;11(4):20–25.
[47] Jame R. Phytochemical and pharmacological uses of *Acacia nilotica* – a review. Seeds. 2018;1:15–21.
[48] Rather LJ, Mohammad F. *Acacia nilotica* (L.): a review of its traditional uses, phytochemistry, and pharmacology. Sustain Chem Pharm. 2015;2:12–30. doi:10.1016/j.scp.2015.08.002
[49] Chaudhuri RG, Paria S. Growth kinetics of sulphur nanoparticles in aqueous surfactant solutions. J Colloid Interface Sci. 2011;354(2):563–569. doi:10.1016/j.jcis.2010.11.039
[50] Salem NM, Albanna LS, Awwad AM. Green synthesis of sulphur nanoparticles using *Punica granatum* peels and the effects on the growth of tomato by foliar spray applications. Environ Nanotechnol, Monit Manage. 2016;6:83–87. doi:10.1016/j.enmm.2016.06.006
[51] Ragab GA, Saad-Allah KM. Green synthesis of sulphur nanoparticles using *Ocimum basilicum* leaves and its prospective effect on manganese-stressed *Helianthus annuus* (L.) seedlings. Ecotoxicol Environ Saf 2020;191:110242.
[52] Sadek ME, Shabana YM, Sayed-Ahmed K, et al. Antifungal activities of sulfur and copper nanoparticles against cucumber postharvest diseases caused by *Botrytis cinerea* and *Sclerotinia sclerotiorum*. J Fungi. 2022;8:412. doi:10.3390/jof8040412
[53] Baran MF, Acay H. Antimicrobial activity of silver nanoparticles synthesized with extract of tomato plant against bacterial and fungal pathogens. Middle Black Sea J Health Sci. 2019;5(2):67–73. doi:10.19127/mbsjohs.551132
[54] Keskin C, Baran A, Baran MF, et al. Green synthesis, characterization of gold nanomaterials using *Gundelia tournefortii* leaf extract, and determination of their nanomedicinal (antibacterial, antifungal, and cytotoxic) potential. Hindawi J Nanomater. 2022;2022(1):7211066.
[55] Najafi S, Razavi SM, Khoshkam M, et al. Green synthesized of sulphur nanoparticles and its application on lettuce plants metabolic profiling. BioNanoScience. 2022;12(1):116–127. doi:10.1007/s12668-021-00918-2
[56] Khairan K, Jalil Z. Green synthesis of sulphur nanoparticles using aqueous garlic extract (*Allium sativum*). Rasayan J Chem. 2019;12(1):50–57. doi:10.31788/RJC.2019.1214073
[57] Jaiswal L, Shankar S, Rhim JW. Carrageenan-based functional hydrogel film reinforced with sulphur nanoparticles and grapefruit seed extract for wound healing application. Carbohydr Polym. 2019;224:115191. doi:10.1016/j.carbpol.2019.115191

[58] Adamski Z. Studies of a role played by lipophilic yeasts *Malassezia furfur* (*Pityrosporum ovale*, *Pityrosporum orbiculare*) in different dermatoses. Postepy Dermatol (Poznan). 1995;12:349–454.
[59] Ashbee R, Bignell EM. Pathogenic yeast: the yeast handbook. Poland: Poznan (Termedia).
[60] Sawant VJ, Bamane SR, Shejwal RV, et al. Comparison of drug delivery potentials of surface functionalized cobalt and zinc ferrite nanohybrids for curcumin in to MCF-7 breast cancer cells. J Magn Magn Mater. 2016;417:222–229. doi:10.1016/j.jmmm.2016.05.061
[61] Manikyam HK, Joshi SK, Vakadi S, et al. Anticancer activity of terpenoid saponin extract of Psidium guajava on MCF-7 cancer cell line using DAPI and MTT assays. African J Pharm Pharmacol. 2021;15(12):206–211. doi:10.5897/AJPP2020.5216
[62] Skrott Z, Cvek B. Diethyldithiocarbamate complex with copper: the mechanism of action in cancer cells, mini-Rev. Med Chem. 2012;12:1184–1192.
[63] Medici V, Sturniolo GC. Tetrathiomolybdate, a copper chelator for the treatment of Wilson disease, pulmonary fibrosis and other indications. IDrugs. 2008 Aug;11(8):592–506.
[64] Liu H, Zhang Y, Zheng S, et al. Detention of copper by sulfur nanoparticles inhibits the proliferation of A375 malignant melanoma and MCF-7 breast cancer cells. Biochem Biophys Res Commun 2016;477(4):1031–1037. doi:10.1016/j.bbrc.2016.07.026
[65] Shankar S, Pangen R, Park JW, et al. Preparation of sulfur nanoparticles and their antibacterial activity and cytotoxic effect. Mater Sci Eng C. 2018;92:508–517. doi:10.1016/j.msec.2018.07.015.